

Bifurcation analysis with self-excited and hidden attractors for a chaotic jerk system



Tahsin I. Rasul^{a,*}, Rizgar H. Salih^b

^aDepartment of Mathematics, Faculty of Science, Soran University, Soran, Kurdistan Region, Iraq.

^bDepartment of Mathematics, College of Basic Education, University of Raparin, Rania, Kurdistan Region, Iraq.

Abstract

This paper is devoted to investigating the local bifurcation of a chaotic jerk system. The local stability of equilibrium points is analyzed, as well as the existence of transcritical bifurcation at the origin. For the proposed jerk system, the Hopf and Zero-Hopf bifurcations are investigated at the origin. Moreover, a zero-Hopf equilibrium point at the origin is characterized for the system. By using the averaging theory of first order, a limit cycle can be bifurcated from the zero-Hopf equilibrium located at the origin. Liapunov quantities techniques are used to investigate the cyclicity of the system. It is shown that three limit cycles can be bifurcated from the origin. Finally, both self-excited chaotic attractors and hidden chaotic attractors are studied for special cases of the chaotic jerk systems using bifurcation diagrams, Lyapunov exponents, and cross-sections. All results reported in this study have been obtained using Maple software.

Keywords: Transcritical bifurcation, zero hopf, Hopf bifurcation, jerk system, self-excited attractors, hidden attractors.

2020 MSC: 34C23, 34C28, 37D45.

©2024 All rights reserved.

1. Introduction

Chaos theory is one of the most important branches of mathematics that studies the behavior of dynamical systems, which are highly sensitive to initial conditions. The first chaotic system with a hidden attractor was discovered in the Chua system [16, 18]. Hidden attractors have generated incredible interest due to their significance in both theory and engineering [3]. Existing chaotic systems can be classified into two types: hidden attractors and self-excited attractors. A chaotic system is considered to have hidden attractors if its basin of attraction is not connected to the small neighborhoods of any equilibrium point [18]. Conversely, if chaotic systems have a basin of attraction that is connected with one or more unstable equilibrium points, they are referred to as self-excited attractors [15]. Generally, self-excited attractors can be numerically identified from unstable equilibria. On the other hand, hidden attractors are challenging to localize due to the fact that their basin of attraction is not associated with small neighborhoods of any equilibrium points. Hidden attractors have been discovered in various types of nonlinear systems,

*Corresponding author

Email address: tahsin.rasul@soran.edu.iq (Tahsin I. Rasul)

doi: [10.22436/jmcs.035.03.05](https://doi.org/10.22436/jmcs.035.03.05)

Received: 2024-01-28 Revised: 2024-04-12 Accepted: 2024-04-21

including those with one or more stable equilibria [3, 20, 33, 37], systems with a line of equilibria [10], systems with both stable and unstable equilibria [5] and systems with no equilibria [35].

In physics, a jerk differential equation can be represented as the third order dynamics

$$\ddot{x} = f(x, \dot{x}, \ddot{x}), \quad (1.1)$$

where x, \dot{x}, \ddot{x} , and \ddot{x} represent the displacement, velocity, acceleration, and jerk, respectively. It is appropriate to express (1.1) in system notation by introducing two additional phase variables as

$$y = \dot{x} \quad \text{and} \quad z = \dot{y} = \ddot{x}.$$

Therefore, the status variables x, y, z provide a mechanical meaning of displacement, velocity and acceleration, respectively. Thus, the differential equation (1.1) can be transformed into

$$\begin{cases} \dot{x} = y, \\ \dot{y} = z, \\ \dot{z} = j(x, y, z). \end{cases}$$

Many chaotic jerk systems can be found with various forms of $j(x, y, z)$, including absolute value functions, trigonometric functions and power functions. For more details, refer to [29].

Bifurcation analysis is conducted for nonlinear dynamical systems to comprehend how alterations in system parameters affect the qualitative behavior of the systems [4, 28, 32]. There are numerous analytical and numerical methods that can be efficiently used to investigate local and global bifurcations, such as center manifold reduction, normal forms, perturbation techniques, and projection methods [7, 19, 21].

Several jerk systems of this nature have already been considered in the literature and the outcomes have revealed a range of rich and striking phenomena. These include Hopf bifurcation, coexisting bubbles of bifurcation, coexistence of multiple attractors, coexistence of multiple bifurcation modes, symmetry-breaking, period-doubling scenarios, and symmetric properties [12]. In reference [27], the authors investigated various types of bifurcations for the general quadratic jerk system, including saddle-node and transcritical bifurcations. They have also proven that two limit cycles bifurcate from a zero-Hopf equilibrium point. Braun and Mereu [2] obtained a zero-Hopf bifurcation in a chaotic jerk system. Diab et al. [6] investigated zero-Hopf bifurcations of the generalized Genesio differential equation. In their work, they characterized the existence of a zero-Hopf equilibrium point and showed that at most 6 periodic solutions bifurcate from the origin of the system.

Bifurcated periodic orbits from the center for the 3D jerk system were investigated in [24]. The inverse Jacobi multiplier was utilized to find sufficient conditions for the existence of a center. To determine the cyclicity of the system and the number of limit cycles that can bifurcate, the Liapunov quantities technique was employed. It was demonstrated that under two sets of conditions, three periodic solutions can bifurcate from the origin, while under the other sets of conditions, four periodic solutions can bifurcate. The Hopf bifurcation of a 3D chaotic system was studied by the authors in [25]. The stability of the equilibrium points was examined, and the occurrence of the Hopf bifurcation in the system was investigated. Additionally, the center manifold and Liapunov quantities techniques were employed to analyze the cyclicity of the system. It has been confirmed that at most two periodic solutions can bifurcate from the origin. A study on the local stability and codim-1 bifurcations of an arbitrary one-parameter jerk system was conducted by Luazureanu and Cho [17]. In their work, conditions for the appearance of Hopf and fold bifurcations were constructed. A 3-D jerk system with three quadratic nonlinear terms was presented by Bonny et al. [1], and the dynamical properties of the system were demonstrated by utilizing phase portraits, bifurcation diagrams, Lyapunov exponents, multistability, and coexisting attractors.

Wannaboon et al. [34] have presented a jerk system of the following form

$$\begin{cases} \dot{x} = y, \\ \dot{y} = z, \\ \dot{z} = -\alpha[x + y + z - (\tanh(ax + b) + c)]. \end{cases}$$

This system examines chaotic dynamics in terms of a bifurcation diagram, Lyapunov exponents, chaotic attractor, the waveform in the time domain, equilibrium points and the Jacobian matrix. Hu et al. [9] identified mechanisms that lead to the emergence of chaotic attractors in four jerk systems. Furthermore, the discussion also encompasses the associated multistability concerns. Detailed investigations were conducted on two distinct mechanisms, each characterized by unique bifurcation processes, across the four systems. Joshi and Ranjan [11] proposed the following jerk equation with sine hyperbolic nonlinearity:

$$\ddot{x} + \beta\dot{x} + (\alpha + 1)\beta\dot{x} \pm \alpha\beta\gamma \sinh(x) = 0.$$

The existence of a hidden attractor in the presented system was investigated through numerical simulation, along with the exploration of several basic properties of the system. Rajagopal et al. [22] presented the following jerk oscillator with a cosine hyperbolic

$$\ddot{x} - \alpha x + b\dot{x} + \dot{x} + \cosh(x) = 0.$$

This system exhibits a variety of dynamical behaviors by manipulating its two parameters, including one-scroll chaotic attractor, periodic attractor, and coexistence between chaotic and periodic attractors. Kengne et al. [13], considered the following simple 3D autonomous jerk system with a cubic nonlinearity

$$\begin{cases} \dot{x} = y, \\ \dot{y} = az, \\ \dot{z} = x - \gamma y - z - x^3, \end{cases}$$

where a and $\gamma \geq 0$ are tunable parameters. Through bifurcation analysis, it was determined that the system exhibits classical period-doubling leading to chaos, symmetry-restoring crisis scenarios and the presence of multiple coexisting attractors. In 2018, Jacques Kengne et al. [14] presented novel chaotic jerk system, which can be rewritten as

$$\begin{cases} \dot{x}_1 = x_2, \\ \dot{x}_2 = \alpha x_3, \\ \dot{x}_3 = \gamma x_2 - \mu x_3 + x_1 - x_1|x_1|, \end{cases}$$

where α, γ , and $\mu \geq 0$ are control parameters. They observed various dynamic behaviors, including period doubling sequences leading to chaos, symmetry-recovering crises, periodic windows, and coexisting bifurcations. The stability of equilibria and Hopf bifurcation were analyzed using Lyapunov exponents, time series, Poincaré section plots and bifurcation diagrams. Vaidyanathan et al. [30] considered the following chaotic jerk equation with two cubic nonlinearities

$$\frac{d^3x}{dt^3} = -a \frac{d^2x}{dt^2} + x \left(\frac{dx}{dt} \right)^2 - x^3 - bx + c \sin(\dot{x})$$

where a, b , and c are positive parameters. The chaotic features of the system were thoroughly examined by analyzing the eigenvalue structure, Lyapunov exponents and Kaplan-Yorke dimension. Extensive bifurcation analysis revealed new characteristics, such as point reflection symmetry and bistability of chaos. Additionally, an adaptive backstepping controller was proposed to achieve chaos synchronization for the chaotic jerk equation.

In this paper, we consider the following chaotic Jerk system

$$\begin{cases} \dot{x} = y, \\ \dot{y} = z, \\ \dot{z} = -a_1x - a_2y - a_3z + a_4xy + a_5x^2 + a_6y^2 + a_7\text{zerf}(z), \end{cases} \quad (1.2)$$

where a_i ; $i = 1, 2, \dots, 7$ are real parameters and $\text{erf}(z) = \frac{2}{\sqrt{\pi}} \int_0^z e^{-t^2} dt$. The motivation behind this research paper is to investigate the local bifurcation phenomena exhibited by the proposed system. Bifurcations play a crucial role in understanding the qualitative behavior and stability of dynamical systems.

By studying the local stability of equilibrium points and examining the existence of various bifurcations, our aim is to gain insights into the intricate dynamics of the jerk system and uncover any hidden attractors it may possess. The main contribution of this paper lies in the comprehensive analysis of the local bifurcation behavior of the chaotic jerk system. Specifically, our research focuses on local stability analysis, investigation of transcritical, Hopf and Zero-Hopf bifurcations, cyclicity analysis, and studying the chaotic attractors.

This paper is organized as follows. Section 2 analyzes the stability of the equilibrium points. In Section 3, the transcritical bifurcation, Hopf bifurcation, and zero Hopf bifurcation are investigated. The final section focuses on the investigation of chaotic attractors in the system, utilizing bifurcation diagrams, phase portraits, two-sided Poincaré sections, and Lyapunov exponents.

2. The equilibrium points with their stability

Consider the following chaotic jerk system:

$$\begin{cases} \dot{x} = y, \\ \dot{y} = z, \\ \dot{z} = -a_1x - a_2y - a_3z + a_4xy + a_5x^2 + a_6y^2 + a_7\text{zerf}(z), \end{cases} \quad (2.1)$$

where a_i ; $i = 1, 2, \dots, 7$ are real parameters, and $\text{erf}(z) = \frac{2}{\sqrt{\pi}} \int_0^z e^{-t^2} dt$. To find all the equilibrium points of system (2.1), we set \dot{x} , \dot{y} and \dot{z} to zero, resulting in $x = 0$ or $\frac{a_1}{a_5}$, $y = 0$, and $z = 0$. Therefore, the jerk system (2.1) has two equilibrium points: $P_0 = (0, 0, 0)$ and $P_1 = \left(\frac{a_1}{a_5}, 0, 0\right)$.

Now, the stability of equilibrium points of the proposed jerk system is analyzed. The Jacobian matrix of the proposed jerk systems at $(x^*; 0; 0)$ is

$$J = \begin{bmatrix} 0 & 1 & 0 \\ 0 & 0 & 1 \\ 2a_5x^* - a_1 & a_4x^* - a_2 & -a_3 \end{bmatrix},$$

which has characteristic equation

$$\varphi(\lambda) = \lambda^3 + a_3\lambda^2 - (a_4x^* - a_2)\lambda - 2a_5x^* + a_1 = 0. \quad (2.2)$$

When $x^* = 0$, the characteristic equation (2.2) becomes

$$\lambda^3 + a_3\lambda^2 + a_2\lambda + a_1 = 0.$$

According to the Routh-Hurwitz criterion, the origin of the systems is asymptotically stable if $a_1, a_2, a_3 > 0$ and $a_1 < a_2a_3$. Otherwise, the equilibrium point is unstable. When $x^* = \frac{a_1}{a_5}$, the characteristic equation (2.2) is

$$\lambda^3 + a_3\lambda^2 - \frac{(a_1a_4 - a_2a_5)\lambda}{a_5} - a_1 = 0. \quad (2.3)$$

From (2.3), the determinant of the Jacobian matrix is a_1 . If $a_1 > 0$, then at least one of the eigenvalues is positive, this implies that the equilibrium point P_1 is unstable. However, by the Routh-Hurwitz stability criterion, the equilibrium point P_1 is asymptotically stable if and only if $a_1 < 0$, $a_3 > 0$, and $\frac{a_3}{a_5}(a_1a_4 - a_2a_5) < a_1$.

3. Local bifurcation analysis

In this section, the focus will be on the examination of various local bifurcations, including the transcritical, Hopf, and zero Hopf bifurcations.

3.1. Transcritical bifurcation

Consider the following differential equation in \mathbb{R}^n :

$$\dot{x} = f(x, \mu), \quad (3.1)$$

where $\mu \in \mathbb{R}$ is a parameter and f is differentiable. Then, the system (3.1) exhibits a transcritical bifurcation if it satisfies Sotomayor's theorem [7, 21]. This theorem provides sufficient conditions for the existence of a transcritical bifurcation in a dynamical system.

Theorem 3.1 (Sotomayor's theorem). *Consider system (3.1) and let there is a point $p_0 \in \mathbb{R}^n$ such that $f(p_0, \mu) = 0$ for all μ , i.e., p_0 is an equilibrium point of system. Moreover, if $\mu = \mu_0$ assume the following condition satisfies:*

- 1) the Jacobian matrix $J = Df(p_0, \mu_0)$ has a zero eigenvalue with an eigenvector v and J^T has an eigenvector w corresponding to zero eigenvalue;
- 2) J has k eigenvalues with negative real parts and it has $n - 1 - k$ eigenvalues with positive real parts, where $0 \leq k \leq n - 1$;
- 3) $w^T f_\mu(p_0, 0) = 0$;
- 4) $w^T [Df_\mu(p_0, 0)v] \neq 0$;
- 5) $w^T [D_x^2 f(p_0, 0)(v, v)] \neq 0$.

Then system (3.1) exhibits a transcritical bifurcation at the equilibrium p_0 as μ passes through $\mu = 0$.

Theorem 3.2. *Consider the jerk system (2.1) with $a_5 \neq 0$. A transcritical bifurcation occurs at the origin as a_1 passes through zero, provided that $a_3 \neq 0$.*

Proof. The analysis of the transcritical bifurcation occurring in the proposed jerk system (2.1) will be carried out with respect to the parameter a_1 . Thus, we will utilize the notation from Theorem 3.1, set $\mu = a_1$ and $x = (x, y, z) \in \mathbb{R}^3$. The jerk system has two equilibrium points: $x_0 = (0, 0, 0)$ and $x_1 = \left(\frac{a_1}{a_5}, 0, 0\right)$. These equilibrium points collide at the origin when $a_1 = 0$. In addition, when $a_1 = 0$, the Jacobian matrix at the origin is

$$J = Df(0, 0) = \begin{pmatrix} 0 & 1 & 0 \\ 0 & 0 & 1 \\ 0 & -a_2 & -a_3 \end{pmatrix}.$$

It has simple eigenvalue $\lambda = 0$. Indeed, the characteristic polynomial of J is given by

$$\Phi(\lambda) = \lambda^3 + a_3\lambda^2 + a_2\lambda. \quad (3.2)$$

$\Phi(\lambda) = 0$ has simple eigenvalue $\lambda = 0$ with non-zero real part eigenvalues $\lambda_{2,3} = -\frac{a_3}{2} \pm \frac{\sqrt{a_3^2 - 4a_2}}{2}$. Note that the vectors $v = (1, 0, 0)^T$ and $w = (a_2, a_3, 1)^T$ are eigenvectors of the matrix J and J^T corresponding to $\lambda = 0$, respectively. Following Theorem 3.1, we have

$$w^T f_{a_1}(0, 0) = 0, \quad w^T [Df_{a_1}(0, 0)v] = -1 \neq 0, \quad w^T [D^2 f(0, 0)(v, v)] = 2a_5 \neq 0.$$

Thus, all the hypotheses of Theorem 3.1 are satisfied. Therefore, the system displays a transcritical bifurcation at the origin at the bifurcation value $a_1 = 0$. \square

3.2. Zero-Hopf Bifurcation

In this subsection, the zero-Hopf bifurcation for the proposed jerk system is investigated. The possibility of a limit cycle is obtained using the averaging theory of the first order. Consequently, an isolated equilibrium point in the three-dimensional differential system, known as a zero-Hopf equilibrium point, is characterized by one zero eigenvalue and two purely imaginary eigenvalues. Firstly, the zero-Hopf equilibrium point of the system located at the origin is characterized.

Proposition 3.3. *The Jerk system (2.1) exhibits a zero-Hopf equilibrium if and only if the conditions $a_1 = a_3 = 0$ and $a_2 > 0$ are satisfied. In this case, the zero-Hopf equilibrium represents the only equilibrium point of the system, localized at the origin.*

Proof. The Jerk system (2.1) possesses an equilibrium point at $(x^*, 0, 0)$, where $x^* = 0$ or $x = \frac{a_1}{a_5}; a_5 \neq 0$. The characteristic equation of the Jacobian matrix at $(x^*, 0, 0)$ of the system is given by:

$$\lambda^3 + a_3\lambda^2 - (a_4x^* - a_2)\lambda - 2a_5x^* + a_1 = 0.$$

To have a zero-Hopf equilibrium, it is required to have one zero eigenvalue and two purely imaginary eigenvalues. By imposing the condition

$$\lambda(\lambda^2 + \omega^2) = 0,$$

where $\omega > 0$, it is found that $a_1 = a_3 = 0$ and $a_2 = \omega^2$. Therefore, the only zero-Hopf equilibrium point is given by $(0, 0, 0)$. \square

The next theorem is one of our main results in this subsection.

Theorem 3.4. *Assume that $(a_1, a_2, a_3) = (\varepsilon\alpha, \varepsilon\beta + \omega^2, \varepsilon\gamma)$ with ε as a sufficiently small parameter. If $\frac{(\omega^4\gamma^2 - \alpha^2)}{a_5(2\sqrt{\pi}\omega^4a_7 + \pi\omega^2a_6 + \pi a_5)} < 0$, then the jerk system (2.1) exhibits a zero-Hopf bifurcation at the equilibrium point located at the origin of coordinates. Additionally, a limit cycle appears at the origin when $\varepsilon = 0$.*

Proof. If $(a_1, a_2, a_3) = (\varepsilon\alpha, \varepsilon\beta + \omega^2, \varepsilon\gamma)$ with $\varepsilon \ll 1$, then the jerk system (2.1) can be expressed in the following form:

$$\begin{cases} \dot{x} = y, \\ \dot{y} = z, \\ \dot{z} = -\varepsilon\alpha x - (\varepsilon\beta + \omega^2)y - \varepsilon\gamma z + a_4yx + a_5x^2 + a_6y^2 + a_7z\text{erf}(z). \end{cases} \tag{3.3}$$

Re-scaling the variables $(x, y, z) = (\varepsilon X, \varepsilon Y, \varepsilon Z)$, the system mentioned above can be transformed into the following form:

$$\begin{cases} \dot{X} = Y, \\ \dot{Y} = Z, \\ \dot{Z} = -\varepsilon\alpha X - (\beta\varepsilon + \omega^2)Y - \varepsilon\gamma Z + \varepsilon a_4XY + \varepsilon a_5X^2 + \varepsilon a_6Y^2 + a_7Z\text{erf}(\varepsilon Z). \end{cases} \tag{3.4}$$

The linear part of the system (3.4) will be changed to its real Jordan normal form when $\varepsilon = 0$, resulting in the following form:

$$\begin{bmatrix} 0 & -\omega & 0 \\ \omega & 0 & 0 \\ 0 & 0 & 0 \end{bmatrix},$$

where $\omega^2 = a_2$. For doing that, we use the following linear change

$$(X, Y, Z)^T = P(U, V, W)^T, \tag{3.5}$$

where

$$P = \begin{bmatrix} 1 & 0 & 1 \\ 0 & -\omega & 0 \\ -\omega^2 & 0 & 0 \end{bmatrix}.$$

In the new variables (U, V, W) , system (3.4) can be written as

$$\begin{cases} \dot{U} = -\varepsilon a_6 V^2 - a_7 U \operatorname{erf}(\varepsilon \omega^2 U) - \gamma \varepsilon U + \frac{\varepsilon a_4}{\omega} UV + \frac{\varepsilon a_4}{\omega} VW - \frac{\varepsilon a_5}{\omega^2} U^2 - \frac{2\varepsilon a_5}{\omega^2} UW \\ \quad - \frac{\beta \varepsilon}{\omega} V - \omega V - \frac{\varepsilon a_5}{\omega^2} W^2 + \frac{\alpha \varepsilon}{\omega^2} U + \frac{\alpha \varepsilon}{\omega^2} W, \\ \dot{V} = \omega U, \\ \dot{W} = \varepsilon a_6 V^2 + a_7 U \operatorname{erf}(\varepsilon \omega^2 U) + \gamma \varepsilon U - \frac{\varepsilon a_4}{\omega} UV - \frac{\varepsilon a_4}{\omega} VW + \frac{\varepsilon a_5}{\omega^2} U^2 + \frac{2\varepsilon a_5}{\omega^2} UW + \frac{\beta \varepsilon}{\omega} V \\ \quad + \frac{\varepsilon a_5}{\omega^2} W^2 - \frac{\alpha \varepsilon}{\omega^2} U - \frac{\alpha \varepsilon}{\omega^2} W. \end{cases} \tag{3.6}$$

Now, system (3.6) is transformed into cylindrical coordinates (r, θ, W) by introducing a change of variables $U = r \cos(\theta)$ and $V = r \sin(\theta)$, resulting in the following expression:

$$\begin{aligned} \dot{r} &= -\frac{1}{\sqrt{\pi} \omega^2} [(r^2 (-\omega^2 a_6 + a_5) \cos(\theta)^2 + 2r \left(-\frac{\omega a_4 \sin(\theta) r}{2} + \frac{\gamma \omega^2}{2} + a_5 W - \frac{\alpha}{2} \right) \cos(\theta) \\ &\quad - \omega r (a_4 W - \beta) \sin(\theta) + a_6 \omega^2 r^2 + W (a_5 W - \alpha)) \sqrt{\pi} + 2a_7 \omega^4 r^2 \cos(\theta)^2] \cos(\theta) \varepsilon + O(\varepsilon^3) \\ \dot{\theta} &= \omega + \frac{1}{\sqrt{\pi} \omega^2 r} [(r^2 (-\omega^2 a_6 + a_5) \cos(\theta)^2 + 2r \left(-\frac{\omega a_4 \sin(\theta) r}{2} + \frac{\gamma \omega^2}{2} + a_5 W - \frac{\alpha}{2} \right) \cos(\theta) \\ &\quad - \omega r (a_4 W - \beta) \sin(\theta) + a_6 \omega^2 r^2 + W (a_5 W - \alpha)) \sqrt{\pi} + 2a_7 \omega^4 r^2 \cos(\theta)^2] \sin(\theta) \varepsilon \\ &\quad + O(\varepsilon^3) \\ \dot{W} &= \frac{1}{\sqrt{\pi} \omega^2} [(r^2 (-\omega^2 a_6 + a_5) \cos(\theta)^2 + 2r \left(-\frac{\omega a_4 \sin(\theta) r}{2} + \frac{\gamma \omega^2}{2} + a_5 W - \frac{\alpha}{2} \right) \cos(\theta) \\ &\quad - \omega r (a_4 W - \beta) \sin(\theta) + a_6 \omega^2 r^2 + W (a_5 W - \alpha)) \sqrt{\pi} + 2a_7 \omega^4 r^2 \cos(\theta)^2] \varepsilon + O(\varepsilon^3). \end{aligned} \tag{3.7}$$

We choose θ as the new independent variable, then system (3.7) can be written as

$$\begin{aligned} \frac{dr}{d\theta} &= -\frac{1}{\sqrt{\pi} \omega^3} [(r^2 (-\omega^2 a_6 + a_5) \cos(\theta)^2 + 2r \left(-\frac{\omega a_4 \sin(\theta) r}{2} + \frac{\gamma \omega^2}{2} + a_5 W - \frac{\alpha}{2} \right) \cos(\theta) \\ &\quad - \omega r (a_4 W - \beta) \sin(\theta) + a_6 \omega^2 r^2 + W (a_5 W - \alpha)) \sqrt{\pi} + 2a_7 \omega^4 r^2 \cos(\theta)^2] \cos(\theta) \varepsilon + O(\varepsilon^2), \\ \frac{dW}{d\theta} &= \frac{1}{\sqrt{\pi} \omega^3} [(r^2 (-\omega^2 a_6 + a_5) \cos(\theta)^2 + 2r \left(-\frac{\omega a_4 \sin(\theta) r}{2} + \frac{\gamma \omega^2}{2} + a_5 W - \frac{\alpha}{2} \right) \cos(\theta) \\ &\quad - \omega r (a_4 W - \beta) \sin(\theta) + a_6 \omega^2 r^2 + W (a_5 W - \alpha)) \sqrt{\pi} + 2a_7 \omega^4 r^2 \cos(\theta)^2] \varepsilon + O(\varepsilon^2). \end{aligned} \tag{3.8}$$

The system mentioned above can be expressed in the following form:

$$\dot{x} = \varepsilon F(t, x) + \varepsilon^2 H(t, x, \varepsilon),$$

where $t = \theta, x = (r, W)^T$ and $F(\theta, r, W) = \begin{pmatrix} F_1(\theta, r, W) \\ F_2(\theta, r, W) \end{pmatrix}$,

$$\begin{aligned} F_1(\theta, r, W) &= \frac{-1}{\sqrt{\pi} \omega^3} [(2a_7 \omega^4 r^2 \cos(\theta)^2 - \sqrt{\pi} \cos(\theta)^2 \omega^2 a_6 r^2 - \sin(\theta) \sqrt{\pi} \cos(\theta) \omega a_4 r^2 \\ &\quad + \gamma \sqrt{\pi} \cos(\theta) \omega^2 r - \sin(\theta) \sqrt{\pi} \omega a_4 W r + \sqrt{\pi} \cos(\theta)^2 r^2 a_5 + a_6 \omega^2 \sqrt{\pi} r^2 + 2\sqrt{\pi} \cos(\theta) a_5 W r \\ &\quad + \sin(\theta) \sqrt{\pi} \beta \omega r + \sqrt{\pi} a_5 W^2 - \sqrt{\pi} \cos(\theta) \alpha r - \sqrt{\pi} W \alpha) \cos(\theta)], \\ F_2(\theta, r, W) &= \frac{1}{\sqrt{\pi} \omega^3} [2\omega^4 a_7 r^2 \cos(\theta)^2 - \cos(\theta)^2 \sqrt{\pi} \omega^2 a_6 r^2 - \cos(\theta) \sqrt{\pi} \sin(\theta) \omega a_4 r^2 \\ &\quad + \cos(\theta) \sqrt{\pi} \gamma \omega^2 r - \sqrt{\pi} \sin(\theta) \omega a_4 W r + \cos(\theta)^2 \sqrt{\pi} a_5 r^2 + a_6 \omega^2 \sqrt{\pi} r^2 + 2 \cos(\theta) \sqrt{\pi} a_5 W r \\ &\quad + \sqrt{\pi} \beta \omega \sin(\theta) r + \sqrt{\pi} a_5 W^2 - \sqrt{\pi} \alpha \cos(\theta) r - \sqrt{\pi} \alpha W]. \end{aligned}$$

By applying the averaging theorem of the first order in the interval $[0, 2\pi]$, the following results are obtained:

$$g_1(r, W) = -\frac{1}{2\pi} \int_0^{2\pi} F_1(\theta, r, W) d\theta = -\frac{r (\gamma \omega^2 + 2a_5 W - \alpha)}{2\omega^3},$$

$$g_2(r, W) = \frac{1}{2\pi} \int_0^{2\pi} F_2(\theta, r, W) d\theta = \frac{2\sqrt{\pi} \omega^4 a_7 r^2 + a_6 \omega^2 \pi r^2 + 2a_5 \pi W^2 + a_5 \pi r^2 - 2\alpha \pi W}{2\pi \omega^3}.$$

Therefore, the system $g_1(r, W) = g_2(r, W) = 0$, have four solutions, one of them satisfies $r > 0$, namely

$$r^* = \sqrt{-\frac{\pi (\omega^4 \gamma^2 - \alpha^2)}{2a_5 (2\sqrt{\pi} \omega^4 a_7 + \pi \omega^2 a_6 + \pi a_5)}}, \quad W^* = -\frac{\gamma \omega^2 - \alpha}{2a_5}.$$

Computing the Jacobian determinant of g_1, g_2 at this point, we obtain

$$\det \left(\frac{\partial(g_1, g_2)}{\partial(r, W)} \Big|_{(r, W)=(r^*, W^*)} \right) = -\frac{\gamma^2 \omega^4 - \alpha^2}{2\omega^6} \neq 0,$$

under our assumption, it is nonzero. For ε sufficiently small, according to first order averaging theory [31], system (3.8) has a limit cycle $(r(\theta, \varepsilon), W(\theta, \varepsilon))$ satisfying $(r(\theta, \varepsilon), W(\theta, \varepsilon)) \rightarrow (r^*(\theta, \varepsilon), W^*(\theta, \varepsilon))$ if $\varepsilon \rightarrow 0$. Therefore, the following equation

$$(U(\theta, \varepsilon) = r(\theta, \varepsilon) \cos(\theta), V(\theta, \varepsilon) = r(\theta, \varepsilon) \sin(\theta), W(\theta, \varepsilon)),$$

provides the limit cycle system (3.6). By reverting back to the system (3.4), we can also find the limit cycle $(X(\theta), Y(\theta), Z(\theta))$ through the change of variables (3.5). Since $(x(\theta), y(\theta), z(\theta)) = (X(\varepsilon\theta), Y(\varepsilon\theta), Z(\varepsilon\theta))$, system (3.3) possesses a limit cycle that approaches the origin as ε approaches zero. Consequently, this represents a limit cycle originating from the zero-Hopf equilibrium point located at the origin of coordinates when ε tends to zero. \square

3.3. Multiple Hopf bifurcation

The Hopf bifurcation is a common phenomenon associated with the appearance or disappearance of a limit cycle near an equilibrium point. It can be investigated using various techniques, such as bifurcation formulas [8], Lyapunov quantities [23], and focus quantities [26]. In this subsection, we examine the cyclicity of the system (2.1) by employing Lyapunov quantities techniques to determine the number of limit cycles that can bifurcate from the Hopf points. Due to the computational load for computing Liapunove quantities, only the first three Lyapunove quantities were found.

In general, we can not analysis cyclicity for the three dimensional jerk system (2.1). Therefore, in the next theorem, we try to take a special case.

Theorem 3.5. *Three limit cycles can bifurcate from the equilibrium point at the origin when the parameters in system (2.1) satisfy the conditions $a_3 = \frac{a_1}{a_2}, a_2 > 0, a_1 \neq 0$ with*

- i. $\Omega \neq 0$, which is defined in equation (3.13);
- ii. $\eta_{4|_{b_5^*, b_7^*}} \neq 0$.

Proof. The jacobian matrix of the jerk system (2.1) at the origin is given by

$$J_0 = \begin{bmatrix} 0 & 1 & 0 \\ 0 & 0 & 1 \\ -a_1 & -a_2 & -a_3 \end{bmatrix}.$$

The characteristic equation at the origin is given by

$$\varphi(\lambda, a_3) = \lambda^3 + a_3 \lambda^2 + a_2 \lambda + a_1 = 0. \quad (3.9)$$

When $a_3 = a_3^* = \frac{a_1}{\omega^2}, a_2 = \omega^2, a_1 \neq 0$, where $\omega > 0$, the characteristic equation (3.9) has a pair of purely imaginary eigenvalues $\pm i\omega$ with nonzero eigenvalue $-\frac{a_1}{\omega^2}$. To verify the transversality condition, we can

use the implicit function theorem to obtain the derivative of the complex eigenvalue $\lambda(a_3)$ with respect to a_3 :

$$\frac{d\lambda}{da_3} = \frac{-\frac{\partial f}{\partial a_3}}{\frac{\partial f}{\partial \lambda}} = \frac{\lambda^2}{3\lambda^2 + 2\lambda a_3 + a_2}. \quad (3.10)$$

Substituting $a_3 = a_3^*$, $a_2 = \omega^2$ and $\lambda = i\omega$ into (3.10), we compute

$$\frac{d\operatorname{Re}(\lambda)}{da_3} \Big|_{\{a_3=a_3^*, a_2=\omega^2, \lambda=i\omega\}} = -\frac{\omega^6}{2(\omega^6 + a_1^2)} \neq 0,$$

which implies that the transversality condition is satisfied. Therefore, Hopf bifurcation takes place at $a_3 = a_3^*$ provided that $a_2 = \omega^2$, $a_1 \neq 0$. By applying the transformation

$$\begin{bmatrix} x \\ y \\ z \end{bmatrix} = \begin{bmatrix} 1 & 0 & \frac{\omega^4}{a_1^2} \\ 0 & -\omega & -\frac{\omega^2}{a_1} \\ -\omega^2 & 0 & 1 \end{bmatrix} \begin{bmatrix} u \\ v \\ w \end{bmatrix},$$

after some calculations, the following system is obtained:

$$\begin{cases} \frac{du}{dt} = -\omega v + b_1 u^2 + b_2 uv + b_3 uw + b_4 v^2 + b_5 vw + b_6 w^2 + b_7 u^4 + b_8 u^3 w + b_9 u^2 w^2 \\ \quad + b_{10} u w^3 + b_{11} w^4, \\ \frac{dv}{dt} = \omega u + \frac{a_1}{\omega^3} (b_1 u^2 + b_2 uv + b_3 uw + b_4 v^2 + b_5 vw + b_6 w^2 + b_7 u^4 + b_8 u^3 w + b_9 u^2 w^2 \\ \quad + b_{10} u w^3 + b_{11} w^4), \\ \frac{dw}{dt} = -\frac{a_1}{\omega^2} w - \frac{a_1^2}{\omega^4} (b_1 u^2 + b_2 uv + b_3 uw + b_4 v^2 + b_5 vw + b_6 w^2 + b_7 u^4 + b_8 u^3 w + b_9 u^2 w^2 \\ \quad + b_{10} u w^3 + b_{11} w^4) \end{cases} \quad (3.11)$$

where $b_1 = -\frac{\omega^4(2\omega^4 a_7 + \sqrt{\pi} a_5)}{\sqrt{\pi}(\omega^6 + a_1^2)}$, $b_2 = \frac{\omega^5 a_4}{\omega^6 + a_1^2}$, $b_3 = -\frac{\omega^6(2\sqrt{\pi}\omega^2 a_5 - \sqrt{\pi} a_1 a_4 - 4a_1^2 a_7)}{a_1^2 \sqrt{\pi}(\omega^6 + a_1^2)}$, $b_4 = \frac{\omega^3 a_1 a_6}{\omega^6 + a_1^2}$, $b_5 = \frac{\omega^9 a_4}{a_1^2(\omega^6 + a_1^2)}$, $b_6 = -\frac{\omega^4(\sqrt{\pi}\omega^8 a_5 - \sqrt{\pi}\omega^6 a_1 a_4 + 2a_1^4 a_7)}{\sqrt{\pi} a_1^4(\omega^6 + a_1^2)}$, $b_7 = \frac{2\omega^{12} a_7}{3\sqrt{\pi}(\omega^6 + a_1^2)}$, $b_8 = -\frac{8\omega^{10} a_7}{3\sqrt{\pi}(\omega^6 + a_1^2)}$, $b_9 = \frac{4\omega^8 a_7}{\sqrt{\pi}(\omega^6 + a_1^2)}$, $b_{10} = -\frac{8\omega^6 a_7}{3\sqrt{\pi}(\omega^6 + a_1^2)}$, and $b_{11} = \frac{2\omega^4 a_7}{3\sqrt{\pi}(\omega^6 + a_1^2)}$. Now, due to the computational load involved in obtaining Liapunov quantities, we are unable to obtain them. More powerful computing devices are required for this task. Therefore, we simplify the calculation by fixing and eliminating the parameters a_6 . As a result, the value of b_4 also disappears. In order to investigate the number of limit cycles bifurcating from the equilibrium point, we define the Lyapunov function as follows:

$$F(u, v, w) = u^2 + v^2 + \sum_{k=3}^n \sum_{j=0}^k \sum_{i=0}^j C_{k-j, j-i, i} u^{k-j} v^{j-i} w^i,$$

which satisfies the following equation

$$\chi(F) = \eta_1(u^2 + v^2) + \eta_2(u^2 + v^2)^2 + \dots, \quad (3.12)$$

where χ is the vector field of the system (3.11). By using the computer algebra package MAPLE and solving equation (3.12), we obtain the following linearly independent terms of Liapunov quantities:

1. $\eta_1 = 0$;
2. $\eta_2 = \frac{f_1(a_1, b_i, \omega)}{4\omega^7(4\omega^6 + a_1^2)}$;

$$3. \eta_3 = \frac{f_2(a_1, b_i, \omega)}{96\omega^{15} (4\omega^6 + a_1^2) (36\omega^{18} + 49\omega^{12}a_1^2 + 14\omega^6a_1^4 + a_1^6)};$$

$$4. \eta_4 = f_3(a_1, b_i, \omega)/(9216 (9\omega^{12} + 10\omega^6a_1^2 + a_1^4) (2304\omega^{36} + 13072\omega^{30}a_1^2 + 17336\omega^{24}a_1^4 + 8041\omega^{18}a_1^6 + 1606\omega^{12}a_1^8 + 137\omega^6a_1^{10} + 4a_1^{12}) (4\omega^6 + a_1^2)^2 a_1\omega^{23}),$$

where $f_1(a_1, b_i, \omega)$, $f_2(a_1, b_i, \omega)$, and $f_3(a_1, b_i, \omega)$ are polynomials in a_1, b_i, ω , $i = 1, 2, 3, 5, \dots, 11$. Due to their extensive size, we do not provide the complete form of these polynomials here. They have respective degrees of 14, 42, and 83. To establish the occurrence of three limit cycle bifurcations, it suffices to confirm the existence of a point in the parameter space where f_1 is equal to f_2 , f_3 is not equal to zero and the Jacobian determinant of f_1 , and f_2 at that point is non-zero. The origin is a weak focus of order three for system (3.11) if and only if the following conditions are satisfied:

$$1. b_5 = b_5^* = \frac{1}{\omega^2 a_1^2 (10\omega^6 b_1 + 3\omega^3 a_1 b_2 + a_1^2 b_1)} [4\omega^{12} b_1 b_2 - 8\omega^{11} a_1 b_1 b_3 - 8\omega^9 a_1 b_1^2 + 2\omega^8 a_1^2 b_2 b_3 - 3\omega^6 a_1^2 b_1 b_2 - 5\omega^5 a_1^3 b_1 b_3 - 2\omega^3 a_1^3 b_1^2 - \omega^2 a_1^4 b_2 b_3 - a_1^4 b_1 b_2];$$

$$2. b_7 = b_7^* = -\frac{\partial_1}{\partial_2},$$

where

$$\begin{aligned} \partial_1 = & 8640\omega^{43} b_1^5 b_2^2 - 34560\omega^{42} a_1 b_1^5 b_2 b_3 + 34560\omega^{41} a_1^2 b_1^5 b_2^2 + 324000\omega^{41} a_1^2 b_1^4 b_2 b_3 - 10560\omega^{40} a_1 b_1^6 b_2 \\ & - 42240\omega^{40} a_1 b_1^4 b_2^3 + 141120\omega^{39} a_1^2 b_1^6 b_3 + 233184\omega^{39} a_1^2 b_1^4 b_2^2 b_3 - 302400\omega^{38} a_1^3 b_1^5 b_2 b_6 - 276576\omega^{38} a_1^3 b_1^4 b_2 b_3^2 \\ & + 388800\omega^{37} a_1^4 b_1^5 b_3 b_6 + 78336\omega^{37} a_1^4 b_1^4 b_2^3 + 183600\omega^{38} a_1^3 b_1^3 b_2 b_8 - 13440\omega^{37} a_1^2 b_1^7 + 311688\omega^{37} a_1^2 b_1^5 b_2^2 \\ & - 26376\omega^{37} a_1^2 b_1^3 b_2^4 - 898768\omega^{36} a_1^3 b_1^5 b_2 b_3 + 153696\omega^{36} a_1^3 b_1^3 b_2^3 b_3 + 1036800\omega^{35} a_1^4 b_1^6 b_6 \\ & + 561224\omega^{35} a_1^4 b_1^5 b_2^3 - 159840\omega^{35} a_1^4 b_1^4 b_2^2 b_6 - 214008\omega^{35} a_1^4 b_1^3 b_2^2 b_3^2 + 298080\omega^{34} a_1^5 b_1^4 b_2 b_3 b_6 \\ & + 82560\omega^{34} a_1^5 b_1^3 b_2 b_3^2 + 322200\omega^{35} a_1^4 b_1^4 b_2 b_8 - 9720\omega^{35} a_1^4 b_1^2 b_2^2 b_8 - 662432\omega^{34} a_1^3 b_1^6 b_2 + 259528\omega^{34} a_1^3 b_1^4 b_2^3 \\ & - 2880\omega^{34} a_1^3 b_1^2 b_2^5 + 1221920\omega^{33} a_1^4 b_1^6 b_3 - 678808\omega^{33} a_1^4 b_1^4 b_2^2 b_3 + 18912\omega^{33} a_1^4 b_1^2 b_2^4 b_3 \\ & + 994200\omega^{32} a_1^5 b_1^5 b_2 b_6 + 312272\omega^{32} a_1^5 b_1^4 b_2 b_3^2 + 9144\omega^{32} a_1^5 b_1^3 b_2^3 b_6 - 31008\omega^{32} a_1^5 b_1^2 b_3^2 b_2^2 \\ & + 198360\omega^{31} a_1^6 b_1^5 b_3 b_6 + 78528\omega^{31} a_1^6 b_1^4 b_3^2 + 54072\omega^{31} a_1^6 b_1^3 b_2^2 b_3 b_6 + 19584\omega^{31} a_1^6 b_1^2 b_2^2 b_3^2 + 243420\omega^{32} a_1^5 b_1^3 b_2 b_8 \\ & - 20412\omega^{32} a_1^5 b_1 b_2^3 b_8 + 368032\omega^{31} a_1^4 b_1^7 - 627700\omega^{31} a_1^4 b_1^5 b_2^2 + 64738\omega^{31} a_1^4 b_1^3 b_2^4 + 270\omega^{31} a_1^4 b_1 b_2^6 \\ & + 832480\omega^{30} a_1^5 b_1^5 b_2 b_3 - 120500\omega^{30} a_1^5 b_1^3 b_2^3 b_3 - 2160\omega^{30} a_1^5 b_1 b_2^5 b_3 + 610960\omega^{29} a_1^6 b_1^6 b_6 + 436212\omega^{29} a_1^6 b_1^5 b_2^3 \\ & + 519148\omega^{29} a_1^6 b_1^4 b_2^2 b_6 + 22898\omega^{29} a_1^6 b_1^3 b_2^2 b_3^2 + 7884\omega^{29} a_1^6 b_1^2 b_2^4 b_6 + 6126\omega^{29} a_1^6 b_1 b_2^4 b_3^2 + 19548\omega^{28} a_1^7 b_1^4 b_2 b_3 b_6 \\ & + 76608\omega^{28} a_1^7 b_1^3 b_2 b_3^2 + 11052\omega^{28} a_1^7 b_1^2 b_2^3 b_3 b_6 - 4032\omega^{28} a_1^7 b_1 b_2^3 b_3^2 + 98220\omega^{29} a_1^6 b_1^4 b_8 \\ & + 63558\omega^{29} a_1^6 b_1^2 b_2^2 b_8 - 2916\omega^{29} a_1^6 b_1 b_2 b_8 + 197464\omega^{28} a_1^5 b_1^6 b_2 - 215090\omega^{28} a_1^5 b_1^4 b_2^2 + 1392\omega^{28} a_1^5 b_1^2 b_2^5 \\ & + 729448\omega^{27} a_1^6 b_1^6 b_3 + 254772\omega^{27} a_1^6 b_1^4 b_2^2 b_3 + 14750\omega^{27} a_1^6 b_1^2 b_2^4 b_3 - 270\omega^{27} a_1^6 b_1 b_2^6 b_3 + 467464\omega^{26} a_1^7 b_1^5 b_2 b_6 \\ & + 294330\omega^{26} a_1^7 b_1^4 b_2 b_3^2 + 204970\omega^{26} a_1^7 b_1^3 b_2^3 b_6 - 8350\omega^{26} a_1^7 b_1^2 b_2^3 b_3^2 - 2754\omega^{26} a_1^7 b_1 b_2^5 b_6 + 1530\omega^{26} a_1^7 b_1^5 b_2^3 \\ & + 112008\omega^{25} a_1^8 b_1^5 b_3 b_6 - 804\omega^{25} a_1^8 b_1^4 b_3^2 - 66678\omega^{25} a_1^8 b_1^3 b_2^2 b_3 b_6 + 16200\omega^{25} a_1^8 b_1^2 b_2^2 b_3^2 \\ & + 8478\omega^{25} a_1^8 b_1 b_2^4 b_3 b_6 - 1812\omega^{25} a_1^8 b_1^4 b_2^3 + 66576\omega^{26} a_1^7 b_1^3 b_2 b_8 + 7209\omega^{26} a_1^7 b_1 b_2^3 b_8 + 224224\omega^{25} a_1^6 b_1^7 \\ & - 41402\omega^{25} a_1^6 b_1^5 b_2^2 - 26874\omega^{25} a_1^6 b_1^3 b_2^4 - 936\omega^{25} a_1^6 b_1 b_2^6 + 635712\omega^{24} a_1^7 b_1^5 b_2 b_3 + 92538\omega^{24} a_1^7 b_1^3 b_2^3 b_3 \\ & + 4638\omega^{24} a_1^7 b_1 b_2^5 b_3 + 151888\omega^{23} a_1^8 b_1^6 b_6 + 114442\omega^{23} a_1^8 b_1^5 b_2^2 + 142876\omega^{23} a_1^8 b_1^4 b_2^2 b_6 + 61136\omega^{23} a_1^8 b_1^3 b_2^2 b_3^2 \\ & + 53793\omega^{23} a_1^8 b_1^2 b_2^4 b_6 + 594\omega^{23} a_1^8 b_1 b_2^4 b_3^2 - 729\omega^{23} a_1^8 b_1^6 b_6 + 45864\omega^{22} a_1^9 b_1^4 b_2 b_3 b_6 - 8016\omega^{22} a_1^9 b_1^3 b_2 b_3^3 \\ & - 18387\omega^{22} a_1^9 b_1^2 b_2^3 b_3 b_6 - 2424\omega^{22} a_1^9 b_1 b_2^3 b_3^2 + 1539\omega^{22} a_1^9 b_1^5 b_3 b_6 + 13374\omega^{23} a_1^8 b_1^4 b_8 + 16173\omega^{23} a_1^8 b_1^2 b_2^2 b_8 \\ & + 405\omega^{23} a_1^8 b_1^4 b_8 + 240360\omega^{22} a_1^7 b_1^6 b_2 - 37476\omega^{22} a_1^7 b_1^4 b_2^3 + 786\omega^{22} a_1^7 b_1^2 b_2^5 + 140912\omega^{21} \\ & a_1^8 b_1^6 b_3 + 212695\omega^{21} a_1^8 b_1^4 b_2^2 b_3 + 33089\omega^{21} a_1^8 b_1^2 b_2^4 b_3 + 72\omega^{21} a_1^8 b_1 b_2^6 b_3 + 88342\omega^{20} a_1^9 b_1^5 b_2 b_6 + 60370\omega^{20} a_1^9 b_1^4 b_2 b_2^3 \\ & + 25564\omega^{20} a_1^9 b_1^3 b_2^3 b_6 + 953\omega^{20} a_1^9 b_1^2 b_2^3 b_3^2 + 8154\omega^{20} a_1^9 b_1 b_2^5 b_6 + 207\omega^{20} a_1^9 b_1^5 b_2^3 + 24606\omega^{19} a_1^{10} b_1^5 b_3 b_6 \\ & - 1773\omega^{19} a_1^{10} b_1^4 b_3^2 - 3744\omega^{19} a_1^{10} b_1^3 b_2^2 b_3 b_6 - 5238\omega^{19} a_1^{10} b_1^2 b_2^2 b_3^2 - 54\omega^{19} a_1^{10} b_1 b_2^4 b_3 b_6 \end{aligned}$$

$$\begin{aligned}
 & -549\omega^{19}a_1^{10}b_2^4b_3^3 + 7047\omega^{20}a_1^9b_1^3b_2b_8 + 1782\omega^{20}a_1^9b_1b_2^3b_8 + 43032\omega^{19}a_1^8b_1^7 + 92849\omega^{19}a_1^8b_1^5b_2^2 \\
 & -2005\omega^{19}a_1^8b_1^3b_2^4 + 360\omega^{19}a_1^8b_1b_2^6 + 107016\omega^{18}a_1^9b_1^5b_2b_3 + 34985\omega^{18}a_1^9b_1^3b_2^3b_3 + 5751\omega^{18}a_1^9b_1b_2^5b_3 \\
 & + 18996\omega^{17}a_1^{10}b_1^6b_6 + 11255\omega^{17}a_1^{10}b_1^5b_3^2 + 12309\omega^{17}a_1^{10}b_1^4b_2^2b_6 + 5928\omega^{17}a_1^{10}b_1^3b_2^2b_3^2 + 3753\omega^{17}a_1^{10}b_1^2b_2^4b_6 \\
 & -819\omega^{17}a_1^{10}b_1b_2^4b_3^2 + 594\omega^{17}a_1^{10}b_1^6b_6 + 10089\omega^{16}a_1^{11}b_1^4b_2b_3b_6 - 4398\omega^{16}a_1^{11}b_1^3b_2b_3^3 - 3843\omega^{16}a_1^{11}b_1^2b_2^3b_3b_6 \\
 & -1170\omega^{16}a_1^{11}b_1b_2^3b_3^3 + 162\omega^{16}a_1^{11}b_2^5b_3b_6 + 855\omega^{17}a_1^{10}b_1^4b_8 + 1242\omega^{17}a_1^{10}b_1^2b_2^2b_8 + 81\omega^{17}a_1^{10}b_2^4b_8 \\
 & + 44530\omega^{16}a_1^9b_1^6b_2 + 16324\omega^{16}a_1^9b_1^4b_2^3 + 1944\omega^{16}a_1^9b_1^2b_2^5 + 10466\omega^{15}a_1^{10}b_1^6b_3 + 22727\omega^{15}a_1^{10}b_1^4b_2^2b_3 \\
 & + 2895\omega^{15}a_1^{10}b_1^2b_2^4b_3 + 360\omega^{15}a_1^{10}b_2^6b_3 + 8004\omega^{14}a_1^{11}b_1^5b_2b_6 + 1523\omega^{14}a_1^{11}b_1^4b_2b_3^2 - 2118\omega^{14}a_1^{11}b_1^3b_2^3b_6 \\
 & -1593\omega^{14}a_1^{11}b_1^2b_2^3b_3^2 + 486\omega^{14}a_1^{11}b_1b_2^5b_6 - 72\omega^{14}a_1^{11}b_2^5b_3^2 + 2160\omega^{13}a_1^{12}b_1^5b_3b_6 + 516\omega^{13}a_1^{12}b_1^4b_3^3 \\
 & + 378\omega^{13}a_1^{12}b_1^3b_2^2b_3b_6 - 1800\omega^{13}a_1^{12}b_1^2b_2^2b_3^3 - 810\omega^{13}a_1^{12}b_1b_2^4b_3b_6 - 36\omega^{13}a_1^{12}b_2^4b_3^3 + 294\omega^{14}a_1^{11}b_1^3b_2b_8 \\
 & + 81\omega^{14}a_1^{11}b_1b_2^3b_8 + 3400\omega^{13}a_1^{10}b_1^7 + 13991\omega^{13}a_1^{10}b_1^5b_2^2 + 1717\omega^{13}a_1^{10}b_1^3b_2^4 + 288\omega^{13}a_1^{10}b_1b_2^6 \\
 & + 5755\omega^{12}a_1^{11}b_1^5b_2b_3 - 551\omega^{12}a_1^{11}b_1^3b_2^3b_3 + 180\omega^{12}a_1^{11}b_1b_2^5b_3 + 1168\omega^{11}a_1^{12}b_1^6b_6 + 744\omega^{11}a_1^{12}b_1^5b_2^2 \\
 & + 202\omega^{11}a_1^{12}b_1^4b_2^2b_6 - 2224\omega^{11}a_1^{12}b_1^3b_2^2b_3^2 - 729\omega^{11}a_1^{12}b_1^2b_2^4b_6 - 516\omega^{11}a_1^{12}b_1b_2^4b_3^2 + 27\omega^{11}a_1^{12}b_2^6b_6 \\
 & + 630\omega^{10}a_1^{13}b_1^4b_2b_3b_6 + 252\omega^{10}a_1^{13}b_1^3b_2b_3^3 - 333\omega^{10}a_1^{13}b_1^2b_2^2b_3b_6 - 180\omega^{10}a_1^{13}b_1b_2^3b_3^3 - 81\omega^{10}a_1^{13}b_2^5b_3b_6 \\
 & + 21\omega^{11}a_1^{12}b_1^4b_8 + 27\omega^{11}a_1^{12}b_1^2b_2^2b_8 + 3016\omega^{10}a_1^{11}b_1^6b_2 + 772\omega^{10}a_1^{11}b_1^4b_2^3 + 222\omega^{10}a_1^{11}b_1^2b_2^5 \\
 & + 304\omega^9a_1^{12}b_1^6b_3 - 309\omega^9a_1^{12}b_1^4b_2^2b_3 - 733\omega^9a_1^{12}b_1^2b_2^4b_3 + 18\omega^9a_1^{12}b_2^6b_3 + 322\omega^8a_1^{13}b_1^5b_2b_6 + 432\omega^8a_1^{13}b_1^4b_2b_2^2 \\
 & - 344\omega^8a_1^{13}b_1^3b_2^3b_6 - 613\omega^8a_1^{13}b_1^2b_2^3b_3^2 - 54\omega^8a_1^{13}b_1b_2^5b_6 - 45\omega^8a_1^{13}b_2^5b_3^2 + 66\omega^7a_1^{14}b_1^5b_3b_6 \\
 & - 3\omega^7a_1^{14}b_1^4b_3^3 + 12\omega^7a_1^{14}b_1^3b_2^2b_3b_6 + 54\omega^7a_1^{14}b_1^2b_2^2b_3^3 - 54\omega^7a_1^{14}b_1b_2^4b_3b_6 \\
 & - 3\omega^7a_1^{14}b_2^4b_3^3 + 3\omega^8a_1^{13}b_1^3b_2b_8 + 112\omega^7a_1^{12}b_1^7 + 511\omega^7a_1^{12}b_1^5b_2^2 - 249\omega^7a_1^{12}b_1^3b_2^4 + 18\omega^7a_1^{12}b_1b_2^6 \\
 & + 270\omega^6a_1^{13}b_1^5b_2b_3 - 573\omega^6a_1^{13}b_1^3b_2^3b_3 - 69\omega^6a_1^{13}b_1b_2^5b_3 + 28\omega^5a_1^{14}b_1^6b_6 - 17\omega^5a_1^{14}b_1^5b_2^2 - 11\omega^5a_1^{14}b_1^4b_2^2b_6 \\
 & + 110\omega^5a_1^{14}b_1^2b_2^2b_3^2 - 45\omega^5a_1^{14}b_1^2b_2^4b_6 - 45\omega^5a_1^{14}b_1b_2^4b_3^2 + 9\omega^4a_1^{15}b_1^4b_2b_3b_6 - 6\omega^4a_1^{15}b_1^3b_2b_3^3 \\
 & - 9\omega^4a_1^{15}b_1^2b_2^3b_3b_6 + 6\omega^4a_1^{15}b_1b_2^3b_3^3 + 102\omega^4a_1^{13}b_1^6b_2 - 138\omega^4a_1^{13}b_1^4b_2^3 - 24\omega^4a_1^{13}b_1^2b_2^5 - 10\omega^3a_1^{14}b_1^6b_3 \\
 & + 79\omega^3a_1^{14}b_1^4b_2^2b_3 - 73\omega^3a_1^{14}b_1^2b_2^4b_3 + 4\omega^2a_1^{15}b_1^5b_2b_6 - 11\omega^2a_1^{15}b_1^4b_2b_2^2 - 8\omega^2a_1^{15}b_1^3b_2^3b_6 + 11\omega^2a_1^{15}b_1^2b_2^3b_2^2 \\
 & + 23\omega a_1^{14}b_1^5b_2^2 - 31\omega a_1^{14}b_1^3b_2^4 - 5a_1^{15}b_1^5b_2b_3 + 5a_1^{15}b_1^3b_2^3b_3,
 \end{aligned}$$

$$\begin{aligned}
 \vartheta_2 = & \omega^8 a_1 \left(36\omega^{12} + 13\omega^6 a_1^2 + a_1^4 \right) \left(10\omega^6 b_1 + 3\omega^3 a_1 b_2 + a_1^2 b_1 \right)^2 \left(98\omega^{10} b_1 b_2 - 6\omega^9 a_1 b_1 b_3 + 164\omega^7 a_1 b_1^2 \right. \\
 & \left. + 15\omega^7 a_1 b_2^2 + 51\omega^6 a_1^2 b_2 b_3 + 68\omega^4 a_1^2 b_1 b_2 + 12\omega^3 a_1^3 b_1 b_3 + 20\omega a_1^3 b_1^2 + 9\omega a_1^3 b_2^2 - 3a_1^4 b_2 b_3 \right).
 \end{aligned}$$

Since the Jacobian determinant of the functions η_2, η_3 with respect to b_5, b_7 at $b_5 = b_5^*$ and $b_7 = b_7^*$ is given by

$$\begin{vmatrix} \frac{\partial \eta_2}{\partial b_5} & \frac{\partial \eta_2}{\partial b_7} \\ \frac{\partial \eta_3}{\partial b_5} & \frac{\partial \eta_3}{\partial b_7} \end{vmatrix} = \Omega \neq 0,$$

where

$$\begin{aligned}
 \Omega = & \frac{a_1^2}{96\omega^{10} (4\omega^6 + a_1^2)} [98\omega^{10} b_1 b_2 - 6\omega^9 a_1 b_1 b_3 + 164\omega^7 a_1 b_1^2 + 15\omega^7 a_1 b_2^2 + 51\omega^6 a_1^2 b_2 b_3 \\
 & + 68\omega^4 a_1^2 b_1 b_2 + 12\omega^3 a_1^3 b_1 b_3 + 20\omega a_1^3 b_1^2 + 9\omega a_1^3 b_2^2 - 3a_1^4 b_2 b_3],
 \end{aligned} \tag{3.13}$$

and $\eta_{4|b_5^*, b_7^*}$ is non zero, then by suitable perturbation of the coefficients of Liapunov quantities, three limit cycles can be bifurcated from the origin of system (2.1) in the neighborhood of the equilibrium point. \square

4. Route to self-excited and hidden chaotic attractors

In order to understand the chaotic mechanisms of the system through theoretical analysis and numerical simulations, we consider the special case of the Jerk system (2.1) by fixing some of the parameters

and adding the parameter μ . The studied system in this section will be represented by the following equations:

$$\dot{x} = y, \quad \dot{y} = z, \quad \dot{z} = \mu - \alpha_1 x - 1.55y - 1.13z + xy - 0.33x^2 - 2.5z \operatorname{erf}(z). \quad (4.1)$$

When the system parameters are varied, the system generates different periodic and chaotic attractors. Let $I_1 = [1.5, 2.3]$, $I_2 = [1.5, 1.7515]$, and $I_3 = [1.7515, 2.6]$. We have chosen the parameter α_1 as the only bifurcation parameter with variable $x(t)$. In fact, the following results can be obtained by changing the parameter α_1 with the initial condition $(x(0), y(0), z(0)) = (-1, -0.5, -0.5)$.

4.1. Self-excited chaotic attractor when $\mu = 0.22$ and $\alpha_1 \in I_1$.

Consider the system (4.1) with $\mu = 0.22$ and suppose that α_1 is the parameter varying within the range of I_1 . The system has two unstable equilibrium points at $x = -\frac{50\alpha_1}{33} \pm \frac{\sqrt{2500\alpha_1^2 + 726}}{33}$ and $y = z = 0$. The system generates a self-excited chaotic attractor with the point attractor for $\alpha_1 = 1.60$ and $\alpha_1 = 2$ as shown in Fig. 1. To illustrate the folding and stretching structure of the attractor, cross-sections (two-side Poincaré sections) are displayed in Fig. 2.

The Lyapunov exponents of the attractor were calculated utilizing the Wolf's algorithm as described in [36], using the ode45 solver in MATLAB with a time-step of 0.05 for a total simulation duration of 30000 units. The attractor has Lyapunov exponents when $\alpha_1 = 1.60$ as $L_1 = 0.0821$, $L_2 = 0$, and $L_3 = -1.2005$ and the Kaplan-Yorke dimension is $D_{KY} = 2 + \frac{L_1 + L_2}{|L_3|} = 2.0684$. In addition, the largest Lyapunov exponent (MLE) is positive, indicating that the system is chaos. The sum of all Lyapunov exponents is negative, implying that the system is dissipative.

The bifurcation diagram depicting local extrema of $x(t)$ and the Lyapunov exponent versus the parameter α_1 is plotted in Fig. 3 (a) and (b), respectively. From Fig. 3 (a), it can be observed that the system exhibits two chaotic regions: one for $1.5 \leq \alpha_1 \leq 1.71$ and another for $1.72 \leq \alpha_1 \leq 2.3$. The first region follows a period-halving route to exit chaos, showing several periodic windows, while the second region undergoes period doubling, resulting in oscillations with higher periods and exits with inverse period doubling accompanied by periodic windows. Fig. 3 (b) shows the corresponding Lyapunov exponents with respect to the parameter α_1 .

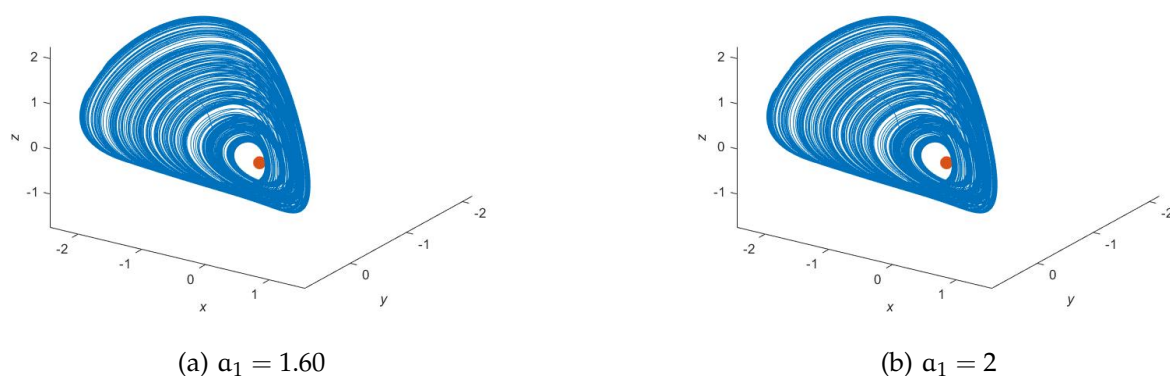


Figure 1: 3D self-excited chaotic attractor of system (4.1) with $\mu = 0.22$. Initial condition: $x(0) = -1, y(0) = -0.5, z(0) = -0.5$. Red point: unstable equilibrium.

4.2. Hidden chaotic attractor when $\mu = 0$ and $\alpha_1 \in I_2$

Let's consider system (4.1) with $\mu = 0$ and $\alpha_1 \in I_2$. In the region I_2 , the origin is always asymptotically stable. The bifurcation diagram depicting local extrema of $x(t)$ and the Lyapunov exponent versus parameter α_1 are presented in Fig. 4 (a) and (b), respectively. As can be seen from the bifurcation diagram

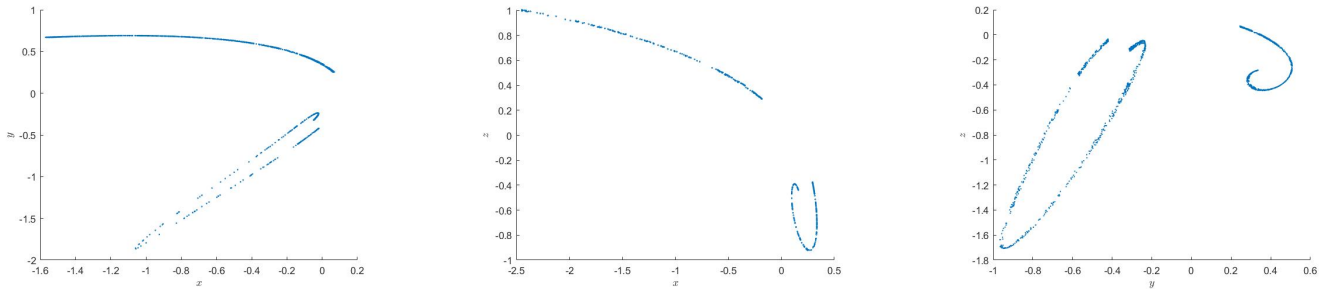


Figure 2: Cross-sections of the chaotic attractor of system (4.1) with $\mu = 0.22$ and $\alpha_1 = 1.60$. Initial condition: $x(0) = -1, y(0) = -0.5, z(0) = -0.5$.

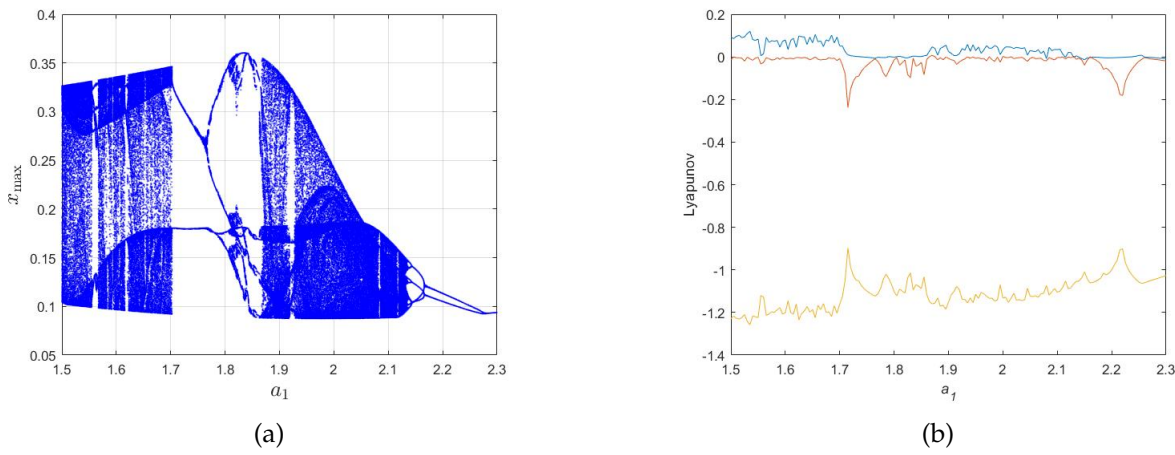


Figure 3: (a) Bifurcation diagram; and (b) Lyapunov exponents spectrum versus α_1 of system (4.1) with initial condition: $(-1, -0.5, -0.5)$.

(see Fig. 4 (a)), at the beginning, the system has a point attractor followed by period-1-oscillations. Then it has grown into period-doubling to chaos interspersed with periodic windows. By further increasing the parameter α_1 , the component $x(t)$ undergoes a hidden chaotic attractor with higher period. Behind the bifurcation diagrams, the corresponding Lyapunov exponents α_1 versus is plotted in Fig. 4 (b).

A hidden chaotic attractor of system (4.1) for $\alpha_1 = 1.69$ is shown in Fig. 5. The cross-sections of the basin of attraction of the attractors are displayed in Fig. 6.

The Lyapunov exponents of the jerk system (4.1) are found for $\alpha_1 = 1.69$ as $L_1 = 0.0729, L_2 = 0, L_3 = -1.2274$. Hence, the maximal Lyapunov exponent (MLE) of the jerk system is positive, implying that the system is chaotic. The sum of these Lyapunov exponents is negative, indicating that the system is dissipative. When the signs of the Lyapunov exponents are $(+, 0, -)$, a strange attractor for the dissipative jerk system is considered. The Kaplan-Yorke dimension of the jerk system is calculated as

$$D_{KY} = 2 + \frac{L_1 + L_2}{|L_3|} = 2.0594.$$

4.3. Self-excited chaotic attractor when $\mu = 0$ and $\alpha_1 \in I_3$

Consider the system (4.1) with $\mu = 0$ and $\alpha_1 \in I_3$. It exhibits two unstable equilibrium points at $(0, 0, 0)$ and $(-3.03030303\alpha_1, 0, 0)$. A self-excited chaotic attractor of the system can be observed when $\alpha_1 = 1.93$, as depicted in Fig. 7. In the proposed system, a cross-section of the basins of attraction of the two attractors in the $y - z$ plane is illustrated in Fig. 8 at $x = 0$. The Lyapunov exponents for the proposed system were computed using the Wolf algorithm, with a total simulation duration of 40000 units and a

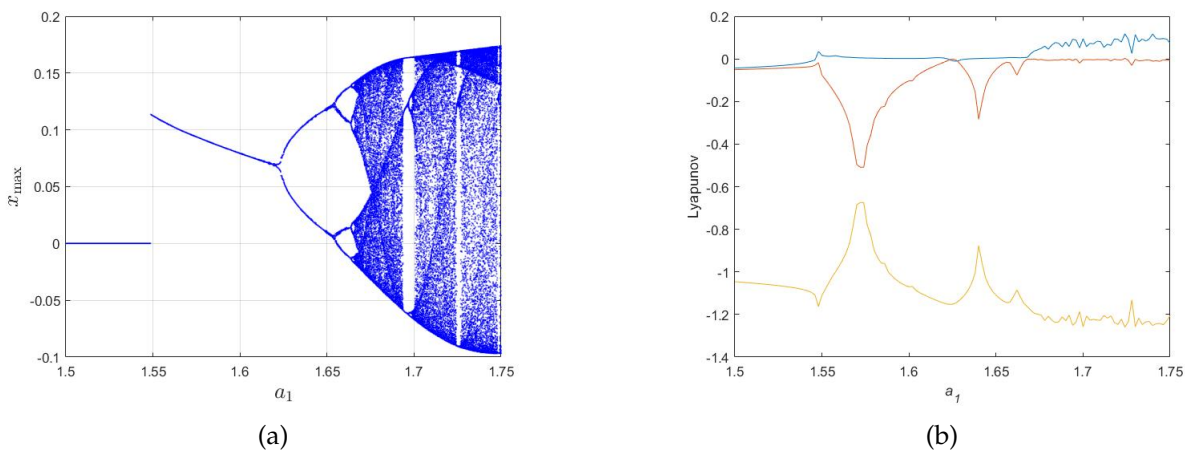


Figure 4: (a) Bifurcation diagram; and (b) Lyapunov exponents spectrum versus a_1 of system (4.1) with $\mu = 0$. Initial condition: $(-1, -0.5, -0.5)$.

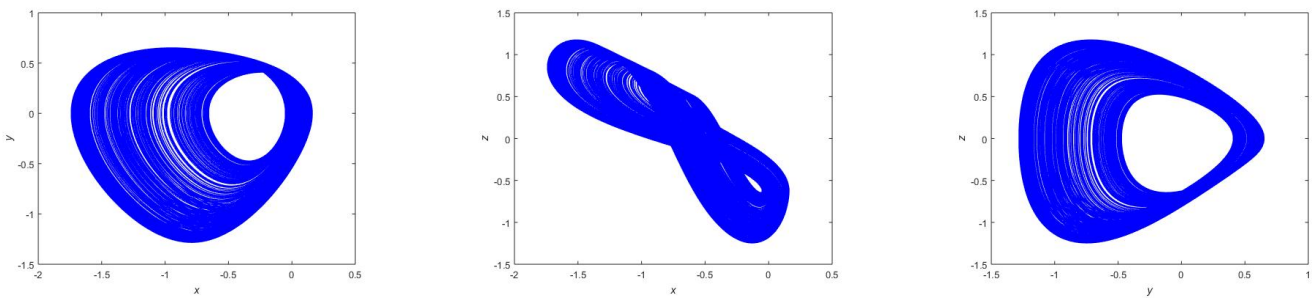


Figure 5: Hidden chaotic attractor of the system (4.1) with $\mu = 0$ and $a_1 = 1.69$.

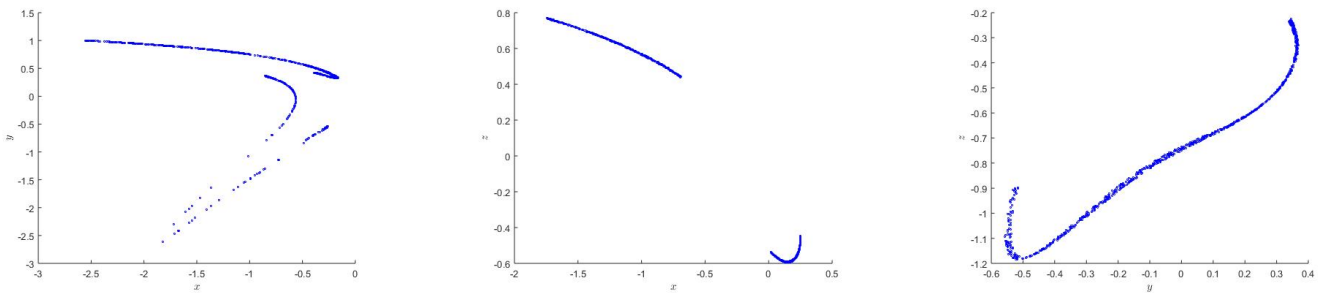


Figure 6: Cross-sections of the chaotic attractor of system (4.1) with $\mu = 0$ and $a_1 = 1.69$.

time-step of 0.5. The computed values are as $L_1 = 0.0486$, $L_2 = 0$, and $L_3 = -1.1388$. The Kaplan-Yorke dimension is found to be 2.0427. The existence of a positive maximum Lyapunov exponent indicates the chaotic nature of the system. Furthermore, the negative sum of all Lyapunov exponents suggests the dissipative nature of the system.

As we all know, bifurcation diagrams and Lyapunov exponent are helpful tools for analyzing the dynamical behaviors of a chaotic system. The bifurcation diagram is shown in Fig. 9 (a) for the system (4.1) with $\mu = 0$, which depicts the local maxima of $x(t)$ versus the parameter a_1 with initial condition $(-1, -0.5, -0.5)$. It can be seen various dynamic properties, including chaos, period-doubling bifurcation routes, period-3 window and other periodic windows. Additionally, as the parameter a_1 increases gradually, the system displays several periodic windows. The chaotic behaviour is confirmed by the Lyapunov exponent displayed in Fig. 9 (b).

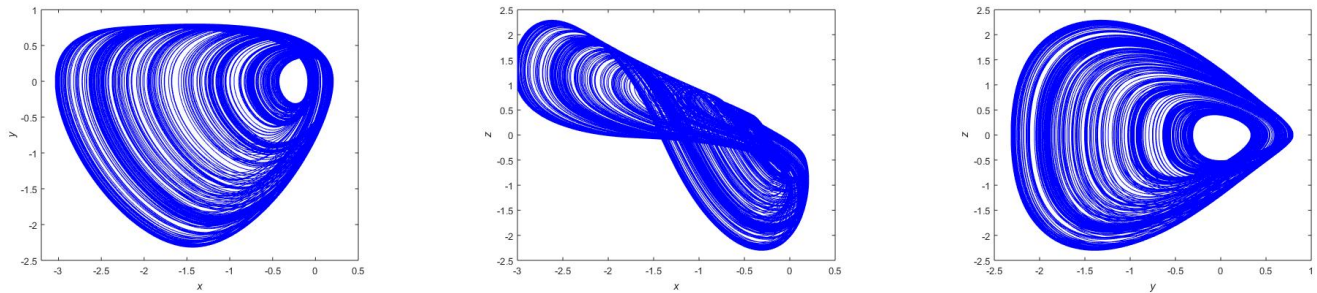


Figure 7: Self-excited attractors of system (4.1) with $\mu = 0$ and $\alpha_1 = 1.93$. Initial condition: $(-1, -0.5, -0.5)$.

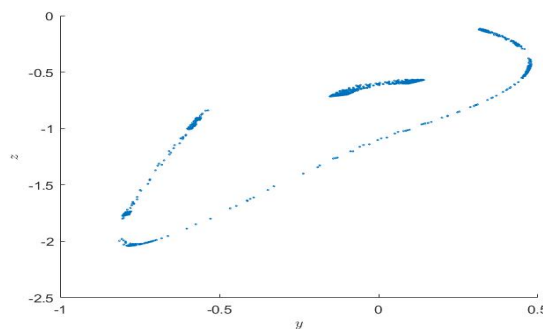


Figure 8: Cross section in the $y - z$ plane (at $x = 0$) of the chaotic attractor of system (4.1) with $\mu = 0$ and $\alpha_1 = 1.93$. Initial condition: $(-1, -0.5, -0.5)$.

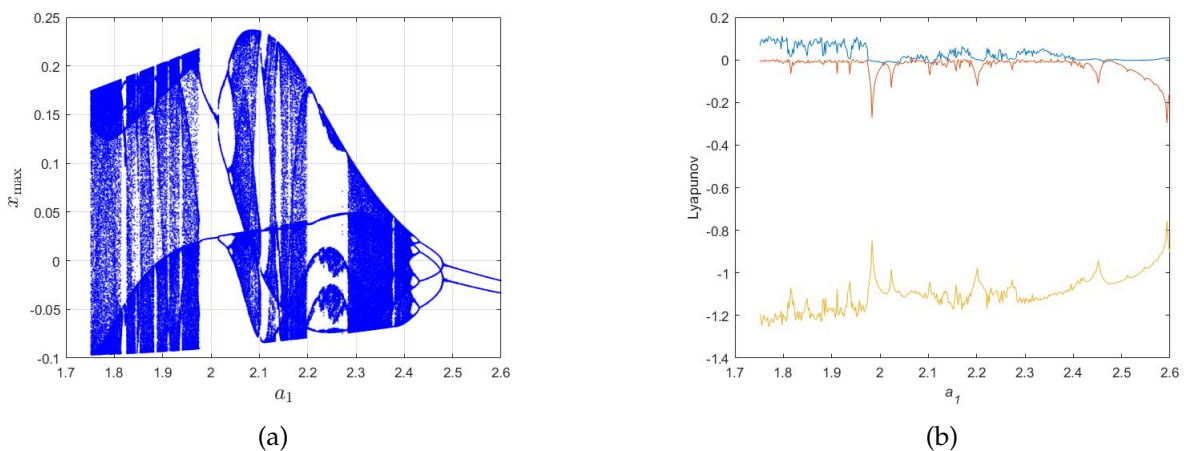


Figure 9: (a) Bifurcation diagram; and (b) Lyapunov exponents spectrum versus α_1 of system (4.1) with $\mu = 0$. Initial condition: $(-1, -0.5, -0.5)$

5. Conclusion

In this paper, the local bifurcation of the equilibrium point at the origin of the chaotic jerk system (2.1) has been investigated. The stability of equilibria and the occurrence of the transcritical bifurcation are studied. Additionally, zero-Hopf and Hopf bifurcations are analyzed. By utilizing the first-order average theory, it has been determined that a single periodic solution emerges from the zero-Hopf equilibrium at the origin. Furthermore, under specific parameter conditions, it has also been verified that three limit cycles can be bifurcated from the origin of the system using Liapunov quantities techniques. In the last section, two types of chaotic attractors are thoroughly examined for a specific case of the chaotic jerk

system by applying phase portraits, bifurcation diagrams, cross-sections, and Lyapunov exponents.

Author's contributions statement

This work is part of Tahsin I. Rasul's PhD study under the supervision of Assistant Professor Dr. Rizgar H. Salih. The research was conducted collaboratively by both authors, who contributed to the design and implementation of the study, analysis of the results, and writing of the manuscript.

References

- [1] T. Bonny, S. Vaidyanathan, A. Sambas, K. Benkouide, W. A. Nassan, O. Naqaweh, *Multistability and bifurcation analysis of a novel 3d jerk system: Electronic circuit design, fpga implementation, and image cryptography scheme*, IEEE Access, **11** (2023), 1–17. 1
- [2] F. Braun, A. C. Mereu, *Zero-Hopf bifurcation in a 3D jerk system*, Nonlinear Anal. Real World Appl., **59** (2021), 8 pages. 1
- [3] S. Cang, Y. Li, R. Zhang, Z. Wang, *Hidden and self-excited coexisting attractors in a Lorenz-like system with two equilibrium points*, Nonlinear Dyn., **95** (2019), 381–390. 1
- [4] Q. Chen, B. Li, W. Yin, X. Jiang, X. Chen, *Bifurcation, chaos and fixed-time synchronization of memristor cellular neural networks*, Chaos Solitons Fractals, **171** (2023), 10 pages. 1
- [5] M.-F. Danca, *Hidden chaotic attractors in fractional-order systems*, Nonlinear Dynam., **89** (2017), 577–586. 1
- [6] Z. Diab, J. L. G. Guirao, J. A. Vera, *Zero-Hopf bifurcation in a generalized Genesio differential equation*, Mathematics, **9** (2021), 1–11. 1
- [7] J. Guckenheimer, P. Holmes, *Nonlinear oscillations, dynamical systems, and bifurcations of vector fields*, Springer-Verlag, New York, (2013). 1, 3.1
- [8] B. D. Hassard, N. D. Kazarinoff, Y. H. Wan, *Theory and applications of Hopf bifurcation*, Cambridge University Press, Cambridge-New York, (1981). 3.3
- [9] X. Hu, B. Sang, N. Wang, *The chaotic mechanisms in some jerk systems*, AIMS Math., **7** (2022), 15714–15740. 1
- [10] S. Jafari, J. C. Sprott, *Simple chaotic flows with a line equilibrium*, Chaos Solitons Fractals, **57** (2013), 79–84. 1
- [11] M. Joshi, A. Ranjan, *An autonomous simple chaotic jerk system with stable and unstable equilibria using reverse sine hyperbolic functions*, Internat. J. Bifur. Chaos Appl. Sci. Engrg., **30** (2020), 10 pages. 1
- [12] L. K. Kengne, H. T. Kamdem Tagne, J. R. Mboupda Pone, J. Kengne, *Dynamics, control and symmetry-breaking aspects of a new chaotic Jerk system and its circuit implementation*, Eur. Phys. J. Plus, **135** (2020). 1
- [13] J. Kengne, Z. T. Njitacke, H. B. Fotsin, *Dynamical analysis of a simple autonomous jerk system with multiple attractors*, Nonlinear Dynam., **83** (2016), 751–765.. 1
- [14] J. Kengne, V. R. F. Signing, J. C. Chedjou, G. D. Leutcho, *Nonlinear behavior of a novel chaotic jerk system: antimonotonicity, crises, and multiple coexisting attractors*, Int. J. Dyn. Control, **6** (2018), 468–485. 1
- [15] N. V. Kuznetsov, *Hidden attractors in fundamental problems and engineering models: A short survey*, Lecture Notes in Electrical Engineering, Springer, Cham, (2016), 13–25. 1
- [16] N. V. Kuznetsov, G. A. Leonov, V. I. Vagaitsev, *Analytical-numerical method for attractor localization of generalized Chua's system*, IFAC Proc. Vol., **43** (2010), 29–33. 1
- [17] C. Lăzureanu, J. Cho, *On Hopf and fold bifurcations of jerk systems*, Mathematics, **11** (2023), 1–15. 1
- [18] G. A. Leonov, N. V. Kuznetsov, V. I. Vagaitsev, *Localization of hidden Chua's attractors*, Phys. Lett. A, **375** (2011), 2230–2233. 1
- [19] J. Li, Y. Liu, Z. Wei, *Zero-Hopf bifurcation and Hopf bifurcation for smooth Chua's system*, Adv. Difference Equ., **2018** (2018), 17 pages. 1
- [20] M. Molaie, S. Jafari, J. C. Sprott, S. M. R. H. Golpayegani, *Simple chaotic flows with one stable equilibrium*, Internat. J. Bifur. Chaos Appl. Sci. Engrg., **23** (2013), 7 pages. 1
- [21] L. Perko, *Differential equations and dynamical systems*, Springer-Verlag, New York, (2013). 1, 3.1
- [22] K. Rajagopal, S. T. Kingni, G. F. Kuate, V. K. Tamba, V.-T. Pham, *Autonomous jerk oscillator with cosine hyperbolic nonlinearity: analysis, FPGA implementation, and synchronization*, Adv. Math. Phys., **2018** (2018), 12 pages. 1
- [23] R. H. Salih, *Hopf bifurcation and centre bifurcation in three dimensional Lotka-Volterra systems*, PhD thesis, Plymouth University, (2015). 3.3
- [24] R. H. Salih, M. S. Hasso, S. H. Ibrahim, *Centre Bifurcations for a Three-Dimensional System with Quadratic Terms*, Zanco J. Pure Appl. Sci., **32** (2020), 62–71. 1
- [25] R. H. Salih, B. M. Mohammed, *Hopf bifurcation analysis of a Chaotic system*, Zanco J. Pure Appl. Sci., **34** (2022), 87–100. 1
- [26] B. Sang, B. Huang, *Bautin bifurcations of a financial system*, Electron. J. Qual. Theory Differ. Equ., **2017** (2017), 22 pages. 3.3
- [27] B. Sang, B. Huang, *Zero-Hopf bifurcations of 3D jerk quadratic system*, Mathematics, **8** (2020), 1–17. 1

- [28] A. Singh, V. S. Sharma, *Codimension-2 bifurcation in a discrete predator–prey system with constant yield predator harvesting*, *Int. J. Biomath.*, **16** (2023), 27 pages. 1
- [29] J. C. Sprott, *Elegant chaos: algebraically simple chaotic flows*, World Scientific Publishing Co., Singapore, (2010). 1
- [30] S. Vaidyanathan, S. T. Kingni, A. Sambas, M. A. Mohamed, M. Mamat, *A new chaotic jerk system with three nonlinearities and synchronization via adaptive backstepping control*, *Int. J. Eng. Technol.*, **7** (2018), 1936–1943. 1
- [31] F. Verhulst, *Nonlinear differential equations and dynamical systems*, Springer-Verlag, Berlin, (2006). 3.2
- [32] H. Wang, G. Ke, J. Pan, Q. Su, *Modeling, dynamical analysis and numerical simulation of a new 3D cubic Lorenz-like system*, *Sci. Rep.*, **13** (2023), 1–15. 1
- [33] X. Wang, V.-T. Pham, S. Jafari, C. Volos, J. M. Munoz-Pacheco, E. Tlelo-Cuautle, *A new chaotic system with stable equilibrium: From theoretical model to circuit implementation*, *IEEE Access*, **5** (2017), 8851–8858. 1
- [34] C. Wannaboon, T. Masayoshi, *An autonomous chaotic oscillator based on hyperbolic tangent nonlinearity*, In: 2015 15th International Symposium on Communications and Information Technologies (ISCIT), IEEE Access, (2015), 323–326. 1
- [35] Z. Wei, *Dynamical behaviors of a chaotic system with no equilibria*, *Phys. Lett. A*, **376** (2011), 102–108. 1
- [36] A. Wolf, J. B. Swift, H. L. Swinney, J. A. Vastano, *Determining Lyapunov exponents from a time series*, *Phys. D*, **16** (1985), 285–317. 4.1
- [37] Q. Yang, L. Yang, B. Ou, *Hidden hyperchaotic attractors in a new 5D system based on chaotic system with two stable node-foci*, *Internat. J. Bifur. Chaos Appl. Sci. Engrg.*, **29** (2019), 21 pages. 1